

# UCSF

## UC San Francisco Previously Published Works

### Title

Soft tissue variations influence HR-pQCT density measurements in a spatially dependent manner

### Permalink

<https://escholarship.org/uc/item/6g5945rn>

### Authors

Wu, Po-Hung  
Gupta, Tanvi  
Chang, Hanling  
[et al.](#)

### Publication Date

2020-09-01

### DOI

10.1016/j.bone.2020.115505

Peer reviewed



Published in final edited form as:

*Bone*. 2020 September ; 138: 115505. doi:10.1016/j.bone.2020.115505.

## Soft tissue variations influence HR-pQCT density measurements in a spatially dependent manner

Po-hung Wu<sup>a</sup>, Tanvi Gupta<sup>a</sup>, Hanling Chang<sup>b,c</sup>, Dmitry Petrenko<sup>b,c</sup>, Anne Schafer<sup>b,c,d</sup>, Galateia Kazakia<sup>a</sup>

<sup>a</sup>Department of Radiology and Biomedical Imaging at China Basin, University of California – San Francisco, 185 Berry Street, Suite 190, Lobby 6, San Francisco, CA 94107, USA

<sup>b</sup>Department of Medicine, University of California – San Francisco, 505 Parnassus Avenue, San Francisco, CA 94143, USA

<sup>c</sup>Endocrine Research Unit, San Francisco Veterans Affairs Health Care System, 4150 Clement St, San Francisco, CA 94121, USA

<sup>d</sup>Department of Epidemiology and Biostatistics, University of California -San Francisco, 550 16th St 2nd floor, San Francisco, CA 94158, USA

### Abstract

**Objective:** Significant weight loss following treatments for obesity undermines bone metabolism and increases bone turnover and fracture incidence. High resolution peripheral quantitative computed tomography (HR-pQCT) is widely used in skeletal health assessment research to provide noninvasive bone parameter measurement (eg. volumetric bone mineral density (vBMD)) with minimal radiation exposure. However, variation in body composition among study groups or longitudinal variations within individuals undergoing significant weight change will generate artifacts and errors in HR-pQCT data. The purpose of this study is to determine the influence of these artifacts on the measurement of vBMD.

**Methods:** We designed a custom-made hydroxyapatite (HA)-polymer phantom surrounded by layers of reusable gel pack and hydrogenated fat to mimic the distal tibia and the surrounding lean and fat tissue. Four different thicknesses of fat were used to mimic the soft tissue of increasingly overweight individuals. We then evaluated how a change in soft tissue thickness influenced image quality and vBMD quantification within total, trabecular, and cortical bone compartments. Based

---

**Corresponding author:** Po-hung Wu, Telephone: 415-353-4903 (office), pohung.wu@ucsf.edu, Mailing address: 185 Berry Street, Suite 350, 396-01-A, Lobby 6, San Francisco, CA 94107, USA .

Credit Author Statement

Po-hung Wu: Phantom Data analysis, Manuscript writing, and data visualization

Tanvi Gupta: Phantom Data Analysis and visualization

Hanling Chang: Phantom design, data collection and analysis

Dimitry Petrenko: Phantom design, data collection and analysis

Anne Schafer: Conceptualization, Methodology, supervision, Reviewing and Editing

Galateia Kazakia: Conceptualization, Methodology, supervision, Reviewing and Editing

**Publisher's Disclaimer:** This is a PDF file of an unedited manuscript that has been accepted for publication. As a service to our customers we are providing this early version of the manuscript. The manuscript will undergo copyediting, typesetting, and review of the resulting proof before it is published in its final form. Please note that during the production process errors may be discovered which could affect the content, and all legal disclaimers that apply to the journal pertain.

on these data, we applied a data correction to previously acquired clinical data in a cohort of gastric bypass patients.

**Results:** In the phantom measurements, total, trabecular, and cortical vBMD increased as soft tissue thickness decreased. The impact of soft tissue thickness on vBMD varied by anatomic quadrant. When applying the soft tissue data correction to a set of clinical data, we found that soft tissue reduction following bariatric surgery can lead to a clinically significant underestimation of bone loss in longitudinal data, and that the effect is most severe in the cortical compartment.

**Conclusion:** HR-pQCT-based vBMD measurement accuracy is influenced by soft tissue thickness and is spatially inhomogeneous. Our results suggest that variations in soft tissue thickness must be considered in HR-pQCT studies, particularly in studies enrolling cohorts with differing body composition or in studies of longitudinal weight change.

### Keywords

Bone mineral density; HR-pQCT; Obesity; Beam-hardening; Scatter; Bariatric Surgery; Weight loss

---

## 1. INTRODUCTION

Obesity is a worldwide health crisis. Adults with obesity suffer from increased prevalence of severe health problems such as diabetes and cardiovascular diseases, resulting in decreased quality of life and increased mortality. Recently, the skeletal health of adults with obesity has become an area of interest in research and medical care. Several studies have indicated that obesity is not protective against fracture, and that fracture risk may actually be higher at peripheral sites in those with higher BMI [1–8]. Further, recent studies suggest that significant weight loss following treatments for obesity (eg. bariatric surgical procedures) also undermines bone metabolism and increases bone turnover and fracture incidence [9–13].

In order to understand the interactions between bone health and weight, medical imaging techniques are utilized for bone density assessment. Dual-energy X-ray absorptiometry (DXA) is the most common imaging modality to evaluate bone health. In DXA, X-ray beams pass through the body along a single projection, and areal bone mineral density (aBMD) is calculated based on X-ray attenuation. However, several studies have demonstrated that aBMD measurement is influenced by soft tissue thickness and composition [14–17].

Quantitative computed tomography (QCT) is an alternative imaging modality to assess bone density. In QCT, X-ray attenuation is calculated along multiple projections and volumetric BMD (vBMD) is calculated from a three-dimensional reconstruction. Because of the volumetric nature of QCT data, bone and soft tissue can be distinguished and analyzed separately. Therefore, QCT is theoretically less susceptible to soft tissue imaging artifacts. However, errors due to beam hardening and reconstruction artifacts have been documented in QCT vBMD measurement in individuals with obesity [17–21].

High resolution peripheral quantitative computed tomography (HR-pQCT) is widely used in skeletal health assessment research. HR-pQCT can noninvasively measure vBMD and bone microstructure within specific bone compartments at the tibia and radius with minimal radiation exposure [22–25]. However, beam hardening and reconstruction artifacts, as in QCT imaging, may potentially influence results in individuals with obesity or significant weight-loss, causing measurement error in vBMD or over- or underestimations of skeletal changes in longitudinal studies [26–28].

The aim of this study is to determine the influence of beam hardening and reconstruction artifacts on the measurement of vBMD in the setting of individuals with obesity or significant weight change, and to apply these findings to the interpretation of clinical data from a longitudinal study of bone health following obesity treatment. In this study, we designed a phantom, a manufactured model of the tibia with varying soft tissue thicknesses to simulate variation in adipose tissue thickness, and quantified the resulting influence on HR-pQCT vBMD measurements in a spatially resolved manner within the cortical and trabecular compartments. We utilized our findings to estimate the influence of acquisition and reconstruction artifacts on longitudinal vBMD measurements acquired from HR-pQCT in a cohort of patients undergoing Roux-en-Y gastric bypass (RYGB) surgery.

## 2. METHODS

### 2.1. Phantom Preparation

A custom-made hydroxyapatite (HA)-polymer phantom, mimicking average dimensions of the human distal tibia, was used in this study (QRM, Mohrendorf, Germany). The phantom consisted of an outer shell and an insert, both 5cm in length, representing the cortical and trabecular compartments, respectively. The density of the HA-polymer shell representing the cortical compartment was 1000 mg HA/cm<sup>3</sup>, which approximates the average density of human cortical tissue. The cortical shell was designed with a step to model two cortical thicknesses: 1.5 mm and 2.0 mm, both with an inner diameter of 32 mm. The density of the insert representing the trabecular compartment was 180 mg HA/cm<sup>3</sup>. A reusable 2 cm thick gel pack (Walgreens Co., Deerfield IL) and hydrogenated fat (Crisco) within sealed plastic enclosures were layered around the HA-polymer phantom to mimic soft tissue (lean and adipose tissue) surrounding bone (Figure 1). The phantom was constructed in four grades representing four thicknesses of adipose tissue, to model different levels of artifact severity (Table 1). The presence of soft tissue outside the imaging field of view (FOV), often unavoidable in patients with obesity, leads to reconstruction artifacts. Therefore we included soft tissue layers thick enough to extend beyond the FOV (Figure 1).

### 2.2. Phantom Image Acquisition

Scanning was performed on a HR-pQCT scanner (XtremeCT, Scanco Medical AG, Brüttisellen, Switzerland) with the standard protocol provided by the manufacturer: 60 kVp source potential, 900  $\mu$ A tube current, 100 ms integration time, 12.6 cm field of view, 110 slices and isotropic voxels of 82  $\mu$ m. For the phantom study, a total of 8 scans were acquired: one set of scans for each grade with cortical thickness 1.5 mm, and a second set with cortical thickness 2.0 mm.

### 2.3. Phantom Image Analysis

Each phantom scan was processed using algorithms provided by the manufacturer (IPL v5.08b, Scanco Medical AG) to automatically segment the trabecular and cortical bone regions as described previously [29,30] (Figure 2). Total, trabecular, and cortical vBMD were calculated in mgHA/ cm<sup>3</sup>. To study how varying soft tissue configurations affect specific regions within the cortical and trabecular compartments, each compartment was divided into four anatomical regions: anterior, posterior, medial, and lateral, based on the coordinates of the scanner (Figure 3) [31].

To evaluate the impact of soft tissue changes on longitudinal measurement of vBMD, a soft tissue specific factor was calculated from the phantom data, according to the following formula:

$$\Delta vBMD_{soft\ tissue} = \frac{vBMD_{post} - vBMD_{pre}}{vBMD_{pre}} \times 100\%$$

where  $vBMD_{soft\ tissue}$  is the change in measured vBMD caused solely by adipose tissue reduction between pre (baseline) and post (follow-up) scans.  $vBMD_{soft\ tissue}$  was calculated for pre scan configurations of Grade 4 (3.5 cm adipose tissue) and Grade 3 (2.0 cm adipose tissue), and for post scan configurations of Grade 2 (1.5 cm adipose tissue) and Grade 1 (1.0 cm adipose tissue).

A change in soft tissue thickness impacts image quality and vBMD quantification by altering image artifacts, including scatter, beam hardening, and noise. To assess the relative impact of these artifacts on our phantom data, two metrics were calculated. First, to quantify the extent of scatter and beam hardening, two regions of interest (ROI) were designed: (1) a 15 pixel wide ring ROI near the outermost portion of the trabecular region, and (2) a 50 pixel radius circle at the center of the trabecular region (Figure 3). The vBMD difference between the outer ring and central circle was used to quantify cupping, the characteristic feature imposed by scatter and beam hardening. Second, to quantify the noise level, the standard deviation of signal intensity within the trabecular region was calculated.

### 2.4. Human Subjects Study

Data for patients with obesity undergoing RYGB were drawn from our previous longitudinal study [9]. In brief, men and women scheduled for RYGB surgery were recruited from academic bariatric surgery centers (the University of California, San Francisco [UCSF] and the San Francisco Veterans Health Care System [SFVAHCS]). Exclusion criteria included perimenopause and use of medications known to influence bone metabolism. A total of 48 participants (38 women and 10 men, mean age =46±12) contributed both preoperative and postoperative data. Participants were scanned just prior to RYGB surgery, 6 months following surgery, and 12 months following surgery. RYGB patient scanning was performed on the same HR-pQCT system with the same scan settings as the phantom acquisition (Figure 4). Scans were examined to confirm that excessive motion artifacts were not present. Longitudinal scans were registered to baseline in a 2D manner using the software provided by manufacturer. Only the common volume of interest (VOI) was used in analysis.

To evaluate the impact of soft tissue changes on the measurement of longitudinal vBMD change in the RYGB study, each baseline and follow-up scan was scored according to the grading system described in Table 1. Of 48 total participants, 5 presented with soft tissue exceeding the FOV at baseline. Four of these were Grade 4 (soft tissue far exceeding FOV), and one was Grade 3 (soft tissue exceeding FOV). As a result of weight loss and better scan positioning, all five subjects presented as Grade 1 (soft tissue within FOV) at their 12 month follow-up. For each subject in this subset, a corrected 12 month longitudinal vBMD change was calculated by adjusting the original measured 12 month vBMD by the corresponding  $vBMD_{soft\ tissue}$ . In the RYGB cohort as a whole, the average cortical thickness was  $1.4 \pm 0.2$  mm, therefore corrections derived from the 1.5 mm phantom were used. Means and standard deviations of original and corrected 12 month longitudinal vBMD change values were calculated. Paired t-tests were performed to compare original baseline and 12 month vBMD values and to compare original and corrected longitudinal vBMD change values for the subset of participants included in this analysis.

### 3. RESULTS

#### 3.1. Phantom vBMD Analysis

Both trabecular and cortical vBMD increased as soft tissue surrounding the phantom decreased in thickness, with the exception of trabecular vBMD from Grade 4 (3.5 cm) to Grade 3 (2.0 cm) (Figure 5). This effect was more severe for thicker cortical bone, as evidenced by a greater dependence of vBMD on soft tissue volume in the 2.0 mm cortical thickness phantom compared to the 1.5 mm cortical thickness phantom. However, this absolute change was small (5–10 mgHA/cm<sup>3</sup>), particularly compared soft tissue effects, and not clinically significant.

The influence of soft tissue volume on trabecular and cortical vBMD varied by anatomic region (Figure 6). From Grade 4 (3.5 cm) to 3 (2.0 cm), trabecular vBMD increased in the medial quadrant but decreased in lateral, anterior and posterior quadrants. From soft tissue Grade 3 (2.0 cm) to 1 (1.0 cm), trabecular vBMD increased in all four quadrants. Inhomogeneity in vBMD measurement effects was also detected in the cortical compartment. From Grade 4 (3.5 cm) to 3 (2.0 cm), vBMD increased in all quadrants with the exception of a decrease in vBMD in the anterior quadrant. From Grade 3 (2.0 cm) to 1 (1.0 cm), cortical vBMD increased in all quadrants.

Variations in soft tissue volume influenced the level of cupping and noise artifacts. Both cupping and noise increased as soft tissue volume increased. In the 1.5 mm cortical thickness phantom, cupping (outer vBMD – central vBMD) decreased from 52.8 to 42.5 mg HA/cm<sup>3</sup> (–19.5%) as soft tissue decreased from Grade 4 (3.5 cm) to 1 (1.0 cm). Noise decreased from 208.4 to 164.1 (–21.2%) as soft tissue decreased from Grade 4 (3.5 cm) to 1 (1.0 cm). Cupping and noise were higher in the 2.0 mm cortical thickness phantom. With 2.0 mm cortical thickness, cupping decreased from 65.9 to 50.7 mg HA/cm<sup>3</sup> (–23.1%) and noise decreased from 220.1 to 177.6 (–19.3%) as soft tissue increased from Grade 4 (3.5 cm) to 1 (1.0 cm).

### 3.2. Human Subjects vBMD Analysis

As reported previously for the entire RYGB cohort [9], vBMD at the tibia decreased during the 12 months following surgery. Total vBMD and cortical vBMD decreased significantly (mean  $\pm$  SD:  $-2.7 \pm 3.1\%$  and  $-1.6 \pm 2.4\%$ ,  $p < 0.0001$ ). Trabecular vBMD also decreased over the 12-month period, ( $-0.5 \pm 3.8\%$ ), but this did not reach significance.

For the subset of subjects included in this analysis, the original data showed that longitudinal vBMD change at the tibia ranged from 3.3% to  $-6.1\%$  (mean  $\pm$  SD:  $-1.6 \pm 3.6$ , No Significance) for total vBMD, 1.2% to  $-2.8\%$  (mean  $\pm$  SD:  $-0.9 \pm 1.6$ , No Significance) for cortical vBMD, and 4.6% to  $-2.2\%$  (mean  $\pm$  SD:  $1.2 \pm 2.8$ , No Significance) for trabecular vBMD (Table 3, Figure 7). None of these longitudinal changes reached statistical significance.

When the  $vBMD_{soft\ tissue}$  correction (Table 2) was applied to the data for the five selected participants with high baseline soft tissue grade, all 12-month vBMD losses increased (Table 3; Figure 7). The corrected 12-month vBMD loss in the total, cortical and trabecular compartment worsened significantly from the original uncorrected vBMD loss (total:  $-1.6\%$  to  $-4.8\%$ ,  $p < 10^{-5}$ ; cortical:  $-0.9\%$  to  $-5.1\%$ ,  $p < 10^{-4}$  trabecular: 1.2% to  $-0.5\%$ ,  $p = 0.006$ ). These results demonstrate that soft tissue reduction over time leads to an underestimation of bone loss in longitudinal data, and that the effect may be most severe in the cortical compartment.

After applying the  $vBMD_{soft\ tissue}$  correction to the five selected participants, the corrected data showed that longitudinal vBMD change was in fact statistically significant except trabecular region. vBMD change at the tibia ranged from 0.1% to  $-9.2\%$  (mean  $\pm$  SD:  $-4.8 \pm 3.6$ ;  $p = 0.04$ ) for total vBMD,  $-3.2\%$  to  $-7.2\%$  (mean  $\pm$  SD:  $-5.1 \pm 1.7$ ,  $p = 0.001$ ) for cortical vBMD, and 3.3% to  $-2.8\%$  (mean  $\pm$  SD:  $-0.5 \pm 3.0$ , No significance) for trabecular vBMD (Table 3, Figure 7).

## 4. Discussion

In this study, a phantom was designed to mimic the distal tibia and surrounding soft tissue and was used to investigate the effect of substantial weight loss on vBMD measurement by HR-pQCT. The results indicate that measured vBMD has an inverse relationship with soft tissue thickness: greater soft tissue thickness will result in lower measured vBMD. Conversely, in the context of weight loss, soft tissue loss over time will result in a measured increase in vBMD even if true vBMD is unchanged. Further, the results of this study show that the extent of vBMD measurement error and its dependence on soft tissue thickness is spatially inhomogeneous, and is different between the cortical and trabecular compartments. Applying these findings to clinical data acquired in a bariatric surgery weight loss cohort, we found that the influence of soft tissue changes on longitudinal vBMD measurement is substantial and must be addressed to accurately quantify bone density changes. These results suggest that variations in soft tissue thickness must be considered in HR-pQCT studies, and particularly in longitudinal weight loss studies or cross-sectional studies enrolling cohorts with varying degrees of obesity.



In CT scanning, several artifacts related to soft tissue variation can influence vBMD measurement. First, a change in the composition of soft tissue surrounding the bone can increase preferential absorption of low energy photons or change the direction of high energy photons [32,33]. The preferential absorption of low energy photons generates beam-hardening artifact [34]. The change of direction of photons generates scatter artifact. Both artifacts can contribute to a “cupping effect” on the reconstructed image, which decreases the grey level of central voxels relative to peripheral voxels and therefore reduces the accuracy of spatial vBMD measurement [35]. In addition, both artifacts can reduce photon counts received by the detector, which further degrades image quality [21]. Increased noise can result in incorrect segmentation, which will also negatively influence bone quality assessment. Second, oversized objects can exceed the field of view. Attenuation absorbed by those soft tissues outside the field of view can be erroneously mapped back to the object inside the field of view, generating a circular artifact on the image [36–38].

Soft tissue thickness and cortical bone thickness both induce artifacts and degrade image quality, which manifest as increased cupping and noise in the trabecular bone compartment. Severe cupping artifact can cause miscalculation of vBMD in both trabecular and cortical regions, leading to an incorrect assessment of bone quality. In our phantom study, increased soft tissue thickness resulted in increased cupping, which then resulted in decreased measured vBMD, illustrating the effect of cupping on vBMD variation.

The results of regional analysis demonstrate that the out-of-field reconstruction artifact has a spatially dependent influence on measured vBMD. In our study, the bright circular artifact caused by out-of-field material occurred consistently at the anteriomedial edge of the image. As a result of the errors in distribution of this additional attenuation load by the reconstruction algorithm, the measured vBMD within the anterior quadrant, which was closest to this region, was elevated for both cortical and trabecular compartments. We found that the out-of-field reconstruction artifact has varying influence on cortical and trabecular bone, at least partially due to their spatial organization relative to the out-of-field material.

One other group has demonstrated that changes in soft tissue surrounding bone will influence HR-pQCT parameters of bone quality. Signe, et. al designed 6 mm and 12 mm fat-tissue layers using vegetable shortening and wrapped them around a calibration phantom as well as patients during HR-pQCT scanning [39]. Consistent with our results, they demonstrated that the density of the phantom and the cortical and trabecular vBMD of human subjects decreased when the fat layer thickness increased. Unique to our study, however, is the specially-designed phantom that simulates the cortical and trabecular compartments of a tibia. This allowed us to more precisely quantify the influence of soft tissue and cortical geometry on vBMD measurement. In addition, the phantom used in our study enabled the reproduction of artifacts seen in practice in human imaging, for example the out-of-field material that is sometimes unavoidable in subjects with obesity. (Fig 5). An additional strength of our study is our regional analysis, which revealed a spatially-dependent effect of the influence of soft tissue on vBMD measurement.

Our study has several limitations. First, we focused on vBMD analysis and did not evaluate the effects of soft tissue on microarchitectural HR-pQCT parameters. Second, sample size of



our human vBMD correction study was small. Despite these limitations, our phantom and clinical results demonstrate the potential magnitude of errors resulting from changes in soft tissue and variations in cortical geometry, and can serve as a reference to help researchers interpret their results.

In conclusion, we designed a realistic bone and soft tissue phantom to analyze the influence of soft tissue and geometry changes on vBMD measured by HR-pQCT. This work is particularly relevant to imaging studies of individuals with obesity and substantial weight change, as well as studies including cohorts with great variation in body habitus. Our results indicate that soft tissue thickness and the extension of material outside the field-of-view will have significant and spatially dependent impacts on measured vBMD.

## Acknowledgements

This study was supported by the National Institutes of Health (NIH): NIH/NIAMS R01AR069670, NIH/NIDDK R01DK107629, NIH/NIAMS P30 AR075055, and the Department of Veterans Affairs 5IK2CX000549.

## REFERENCES:

- [1]. Kim SH, Yi SW, Yi JJ, Kim YM, Won YJ, Association Between Body Mass Index and the Risk of Hip Fracture by Sex and Age: A Prospective Cohort Study, *J. Bone Miner. Res.* 33 (2018) 1603–1611. 10.1002/jbmr.3464. [PubMed: 29750839]
- [2]. Johansson H, Kanis JA, Odén A, McCloskey E, Chapurlat RD, Christiansen C, Cummings SR, Diez-Perez A, Eisman JA, Fujiwara S, Glüer CC, Goltzman D, Hans D, Khaw KT, Krieg MA, Kröger H, Lacroix AZ, Lau E, Leslie WD, Mellström D, Melton LJ, O'Neill TW, Pasco JA, Prior JC, Reid DM, Rivadeneira F, Van Staa T, Yoshimura N, Carola Zillikens M, A meta-analysis of the association of fracture risk and body mass index in women, *J. Bone Miner. Res.* 29 (2014) 223–233. 10.1002/jbmr.2017. [PubMed: 23775829]
- [3]. De Laet C, Kanis JA, Odén A, Johanson H, Johnell O, Delmas P, Eisman JA, Kroger H, Fujiwara S, Garnero P, McCloskey EV, Mellstrom D, Melton LJ, Meunier PJ, Pols HAP, Reeve J, Silman A, Tenenhouse A, Body mass index as a predictor of fracture risk: A meta-analysis, *Osteoporos. Int* 16 (2005) 1330–1338. 10.1007/s00198-005-1863-y. [PubMed: 15928804]
- [4]. El Maghraoui A, Sadni S, El Maataoui A, Majjad A, Rezqi A, Ouzzif Z, Mounach A, Influence of obesity on vertebral fracture prevalence and vitamin D status in postmenopausal women, *Nutr. Metab* 12 (2015). 10.1186/s12986-015-0041-2.
- [5]. Tang X, Liu G, Kang J, Hou Y, Jiang F, Yuan W, Shi J, Obesity and Risk of Hip Fracture in Adults: A Meta-Analysis of Prospective Cohort Studies, *PLoS One.* 8 (2013). 10.1371/journal.pone.0055077.
- [6]. Lv QB, Fu X, Jin HM, Xu HC, Huang ZY, Xu HZ, Chi YL, Wu AM, The relationship between weight change and risk of hip fracture: Meta-analysis of prospective studies, *Sci. Rep.* 5 (2015). 10.1038/srep16030.
- [7]. Pirro M, Fabbriani G, Leli C, Callarelli L, Manfredelli MR, Fioroni C, Mannarino MR, Scarponi AM, Mannarino E, High weight or body mass index increase the risk of vertebral fractures in postmenopausal osteoporotic women, *J. Bone Miner. Metab.* 28 (2010) 88–93. 10.1007/s00774-009-0108-0. [PubMed: 19578807]
- [8]. Compston JE, Watts NB, Chapurlat R, Cooper C, Boonen S, Greenspan S, Pfeilschifter J, Silverman S, Díez-Pérez A, Lindsay R, Saag KG, Netelenbos JC, Gehlbach S, Hooven FH, Flahive J, Adachi JD, Rossini M, Lacroix AZ, Roux C, Sambrook PN, Siris ES, Obesity is not protective against fracture in postmenopausal women: Glow, *Am. J. Med.* 124 (2011) 1043–1050. 10.1016/j.amjmed.2011.06.013. [PubMed: 22017783]
- [9]. Schafer AL, Kazakia GJ, Vittinghoff E, Stewart L, Rogers SJ, Kim TY, Carter JT, Posselt AM, Pasco C, Shoback DM, Black DM, Effects of Gastric Bypass Surgery on Bone Mass and

- Microarchitecture Occur Early and Particularly Impact Postmenopausal Women, *J. Bone Miner. Res.* 33 (2018) 975–986. 10.1002/jbmr.3371. [PubMed: 29281126]
- [10]. Stein EM, Silverberg SJ, Bone loss after bariatric surgery: Causes, consequences, and management, *Lancet Diabetes Endocrinol.* 2 (2014) 165–174. 10.1016/S2213-8587(13)70183-9. [PubMed: 24622720]
- [11]. Yu EW, Lee MP, Landon JE, Lindeman KG, Kim SC, Fracture Risk After Bariatric Surgery: Roux-en-Y Gastric Bypass Versus Adjustable Gastric Banding, *J. Bone Miner. Res.* 32 (2017) 1229–1236. 10.1002/jbmr.3101. [PubMed: 28251687]
- [12]. Harper C, Pattinson AL, Fernando HA, Zibellini J, Seimon RV, Sainsbury A, Effects of obesity treatments on bone mineral density, bone turnover and fracture risk in adults with overweight or obesity, *Horm. Mol. Biol. Clin. Investig.* 28 (2016) 133–149. 10.1515/hmbci-2016-0025.
- [13]. Gagnon C, Schafer AL, Bone Health After Bariatric Surgery, *JBMR Plus.* 2 (2018) 121–133. 10.1002/jbm4.10048. [PubMed: 30283897]
- [14]. Bolotin HH, DXA in vivo BMD methodology: An erroneous and misleading research and clinical gauge of bone mineral status, bone fragility, and bone remodelling, *Bone.* 41 (2007) 138–154. 10.1016/j.bone.2007.02.022. [PubMed: 17481978]
- [15]. Tothill P, Hannan WJ, Cowen S, Freeman CP, Anomalies in the measurement of changes in total-body bone mineral by dual-energy X-ray absorptiometry during weight change, *J. Bone Miner. Res.* 12 (1997) 1908–1921. 10.1359/jbmr.1997.12.11.1908. [PubMed: 9383696]
- [16]. Van Loan MD, Is dual-energy X-ray absorptiometry ready for prime time in the clinical evaluation of body composition?, *Am. J. Clin. Nutr.* 68 (1998) 1155–1156. 10.1093/ajcn/68.6.1155. [PubMed: 9846841]
- [17]. Yu EW, Thomas BJ, Brown JK, Finkelstein JS, Simulated increases in body fat and errors in bone mineral density measurements by DXA and QCT, *J. Bone Miner. Res.* 27 (2012) 119–124. 10.1002/jbmr.506. [PubMed: 21915902]
- [18]. Duerinckx AJ, Macovski A, Polychromatic streak artifacts in computed tomography images, *J. Comput. Assist. Tomogr.* 2 (1978) 481–487. 10.1097/00004728-197809000-00020. [PubMed: 701528]
- [19]. Joseph PM, Spital RD, A method for correcting bone induced artifacts in computed tomography scanners, *J. Comput. Assist. Tomogr.* 2 (1978) 100–108. 10.1097/00004728-197801000-00017. [PubMed: 670461]
- [20]. Brooks RA, Di Chiro G, Beam hardening in X-ray reconstructive tomography, *Phys. Med. Biol.* 21 (1976) 390–398. 10.1088/0031-9155/21/3/004. [PubMed: 778862]
- [21]. Boas FE, Fleischmann D, CT artifacts: causes and reduction techniques, *Imaging Med.* 4 (2012) 229–240. 10.2217/iim.12.13.
- [22]. Nishiyama KK, Shane E, Clinical imaging of bone microarchitecture with HR-pQCT, *Curr. Osteoporos. Rep.* 11 (2013) 147–155. 10.1007/s11914-013-0142-7. [PubMed: 23504496]
- [23]. Boutroy S, Bouxsein ML, Munoz F, Delmas PD, In vivo assessment of trabecular bone microarchitecture by high-resolution peripheral quantitative computed tomography, *J. Clin. Endocrinol. Metab.* 90 (2005) 6508–6515. 10.1210/jc.2005-1258. [PubMed: 16189253]
- [24]. Kazakia GJ, Hyun B, Burghardt AJ, Krug R, Newitt DC, De Papp AE, Link TM, Majumdar S, In vivo determination of bone structure in postmenopausal women: A comparison of HR-pQCT and high-field MR imaging, *J. Bone Miner. Res.* 23 (2008) 463–474. 10.1359/jbmr.071116. [PubMed: 18052756]
- [25]. Burghardt AJ, Kazakia GJ, Ramachandran S, Link TM, Majumdar S, Age- and gender-related differences in the geometric properties and biomechanical significance of intracortical porosity in the distal radius and tibia, *J. Bone Miner. Res.* 25 (2010) 983–993. 10.1359/jbmr.091104. [PubMed: 19888900]
- [26]. MacNeil JA, Boyd SK, Accuracy of high-resolution peripheral quantitative computed tomography for measurement of bone quality, *Med. Eng. Phys.* 29 (2007) 1096–1105. 10.1016/j.medengphy.2006.11.002. [PubMed: 17229586]
- [27]. Mulder L, Koolstra JH, Van Eijden TMGJ, Accuracy of microCT in the quantitative determination of the degree and distribution of mineralization in developing bone, *Acta Radiol* 45 (2004) 769–777. 10.1080/02841850410008171. [PubMed: 15624521]

- [28]. Fajardo RJ, Cory E, Patel ND, Nazarian A, Laib A, Manoharan RK, Schmitz JE, DeSilva JM, MacLatchy LM, Snyder BD, Bouxsein ML, Specimen size and porosity can introduce error into  $\mu$ CT-based tissue mineral density measurements, *Bone*. 44 (2009) 176–184. 10.1016/j.bone.2008.08.118. [PubMed: 18822398]
- [29]. Kazakia GJ, Tjong W, Nirody JA, Burghardt AJ, Carballido-Gamio J, Patsch JM, Link T, Feeley BT, Benjamin Ma C, The influence of disuse on bone microstructure and mechanics assessed by HR-pQCT, *Bone*. 63 (2014) 132–140. 10.1016/j.bone.2014.02.014. [PubMed: 24603002]
- [30]. Burghardt AJ, Buie HR, Laib A, Majumdar S, Boyd SK, Reproducibility of direct quantitative measures of cortical bone microarchitecture of the distal radius and tibia by HR-pQCT, *Bone*. 47 (2010) 519–528. 10.1016/j.bone.2010.05.034. [PubMed: 20561906]
- [31]. Kazakia GJ, Nirody JA, Bernstein G, Sode M, Burghardt AJ, Majumdar S, Age- and gender-related differences in cortical geometry and microstructure: Improved sensitivity by regional analysis, *Bone*. 52 (2013) 623–631. 10.1016/j.bone.2012.10.031. [PubMed: 23142360]
- [32]. Paul NS, Kashani H, Odedra D, Ursani A, Ray C, Rogalla P, The influence of chest wall tissue composition in determining image noise during cardiac CT, *Am. J. Roentgenol.* 197 (2011) 1328–1334. 10.2214/AJR.11.6816. [PubMed: 22109286]
- [33]. Abazid RM, Smettei OA, Almeman A, Sayed S, Alsaqqa H, Abdelmageed SM, Alharbi FJ, Alhabib AM, Al-Mallah MH, Fat volume measurements as a predictor of image noise in coronary computed tomography angiography, *J. Saudi Hear. Assoc.* 31 (2019) 32–40. 10.1016/j.jsha.2018.11.001.
- [34]. Meganck JA, Kozloff KM, Thornton MM, Broski SM, Goldstein SA, Beam hardening artifacts in micro-computed tomography scanning can be reduced by X-ray beam filtration and the resulting images can be used to accurately measure BMD, *Bone*. 45 (2009) 1104–1116. 10.1016/j.bone.2009.07.078. [PubMed: 19651256]
- [35]. Joseph PM, Spital RD, The effects of scatter in X-ray computed tomography, *Med. Phys.* 9 (1982) 464–472. 10.1118/1.595111. [PubMed: 7110075]
- [36]. Barrett JF, Keat N, Artifacts in CT: Recognition and avoidance, *Radiographics*. 24 (2004). 10.1148/rg.246045065.
- [37]. Cheung JP, Shugard E, Mistry N, Pouliot J, Chen J, Evaluating the impact of extended field-of-view CT reconstructions on CT values and dosimetric accuracy for radiation therapy, *Med. Phys.* 46 (2019) 892–901. 10.1002/mp.13299. [PubMed: 30457170]
- [38]. Ohnesorge B, Flohr T, Schwarz K, Heiken JP, Bae KT, Efficient correction for CT image artifacts caused by objects extending outside the scan field of view, *Med. Phys.* 27 (2000) 39–46. 10.1118/1.598855. [PubMed: 10659736]
- [39]. Caksa S, Yuan A, Rudolph SE, Yu EW, Popp KL, Bouxsein ML, Influence of soft tissue on bone density and microarchitecture measurements by high-resolution peripheral quantitative computed tomography, *Bone*. 124 (2019) 47–52. 10.1016/j.bone.2019.04.008. [PubMed: 30998999]

**Highlight**

- Designed a phantom to mimic tibia and surrounding soft tissue variation
- vBMD measured by HR-pQCT increased as soft tissue thickness decreased.
- The impact of soft tissue thickness on vBMD measured by HR-pQCT varied spatially.
- Soft tissue reduction after RYGB surgery can cause underestimation of bone loss

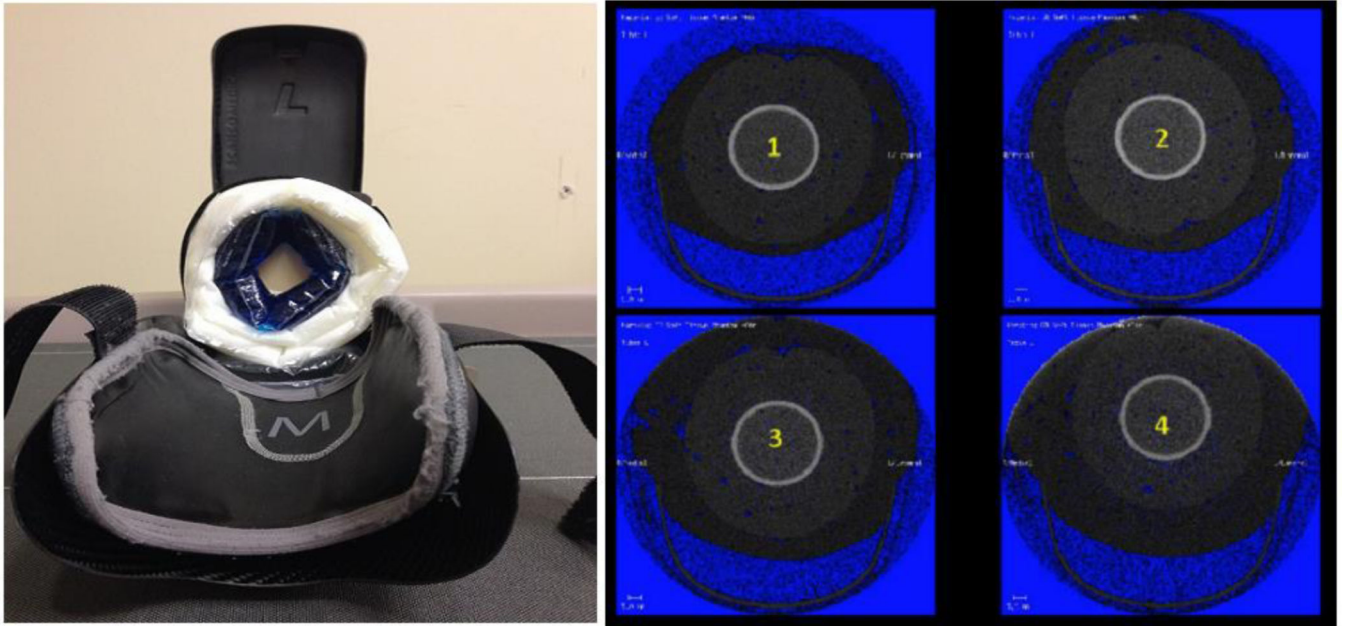


**Figure 1:**  
Soft tissue phantom model. Left: The hydroxyapatite trabecular and cortical phantom surrounded by a gel pack and layers of fat. Right: Four configurations of soft tissue phantoms developed to span the range of artifact severity.

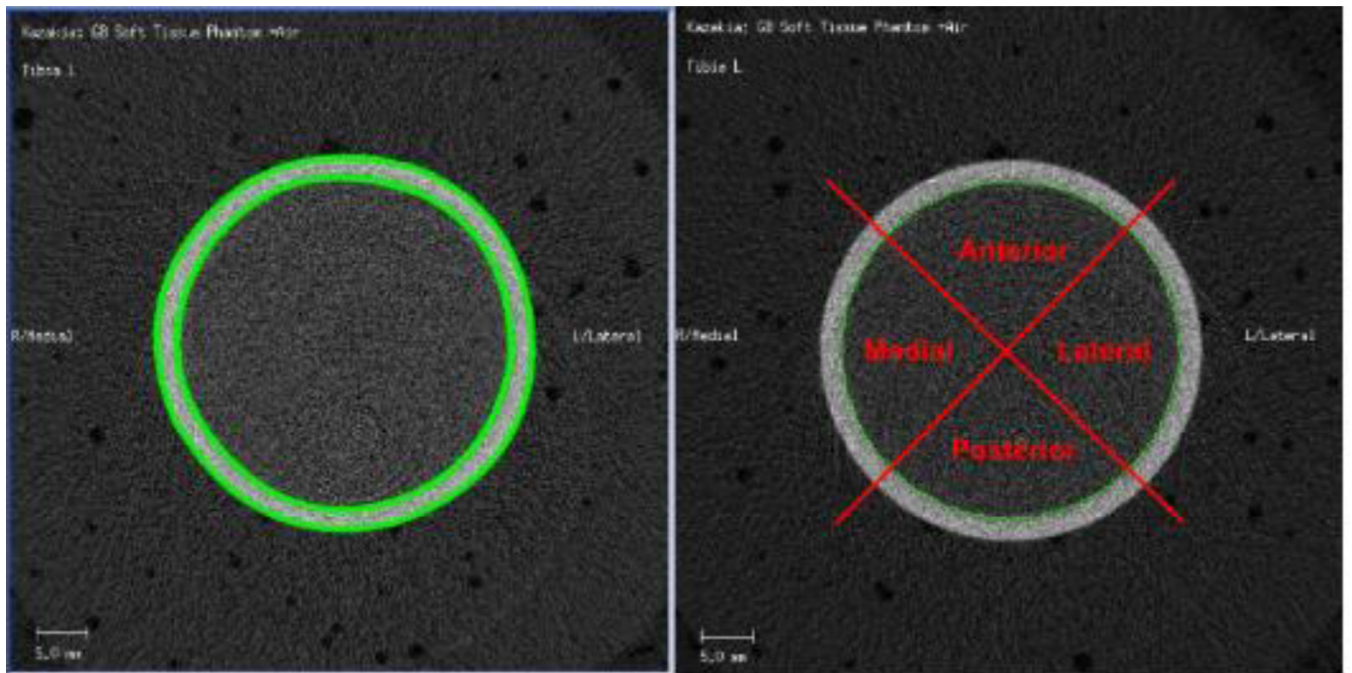


**Figure 2:**  
Contours of cortical and trabecular bone (left) and four anatomical regions (right)

Author Manuscript

Author Manuscript

Author Manuscript

Author Manuscript



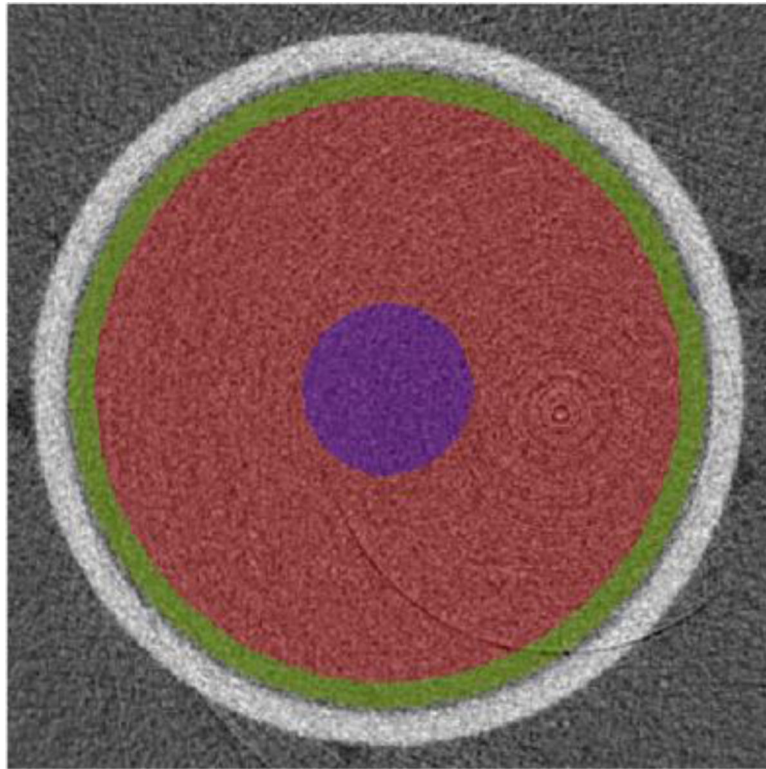


**Figure 3:** Example of ROI for artifact analysis. The outer ring (green) and central circle (blue) are within the trabecular compartment. Mean vBMD was calculated for the outer ring and central circle, and the difference was used to characterize the impact of the cupping artifact.



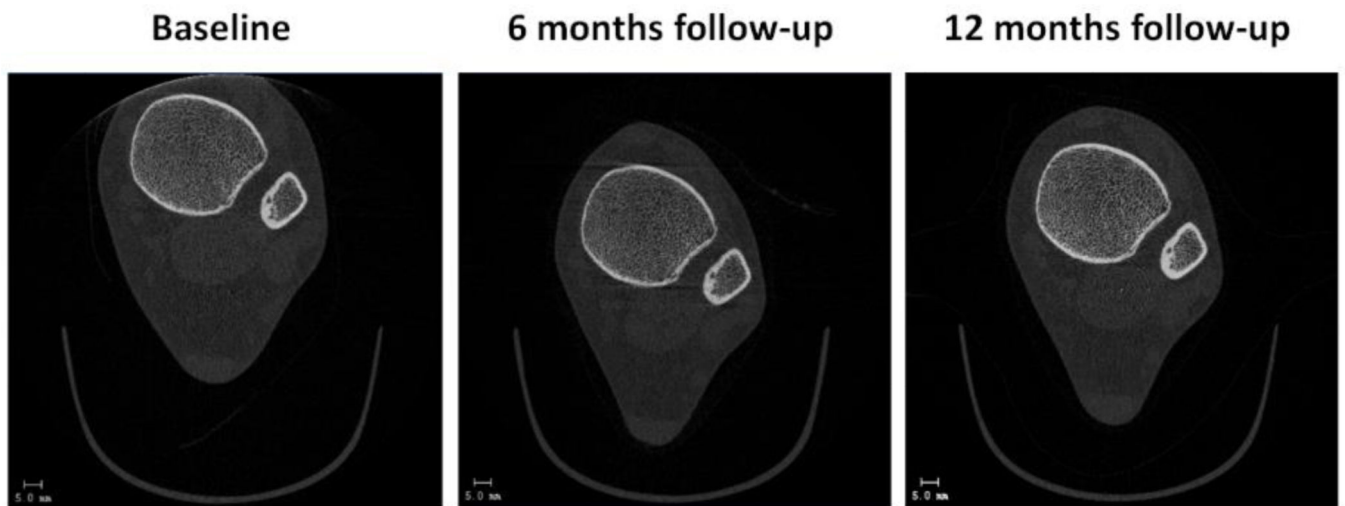


**Figure 4:** HR-pQCT scans from the RYGB study. In the baseline scan, poor positioning due to excess soft tissue resulted in soft tissue exceeding the field of view, and the resulting reconstruction error is visible as a bright streak at the field of view edge.

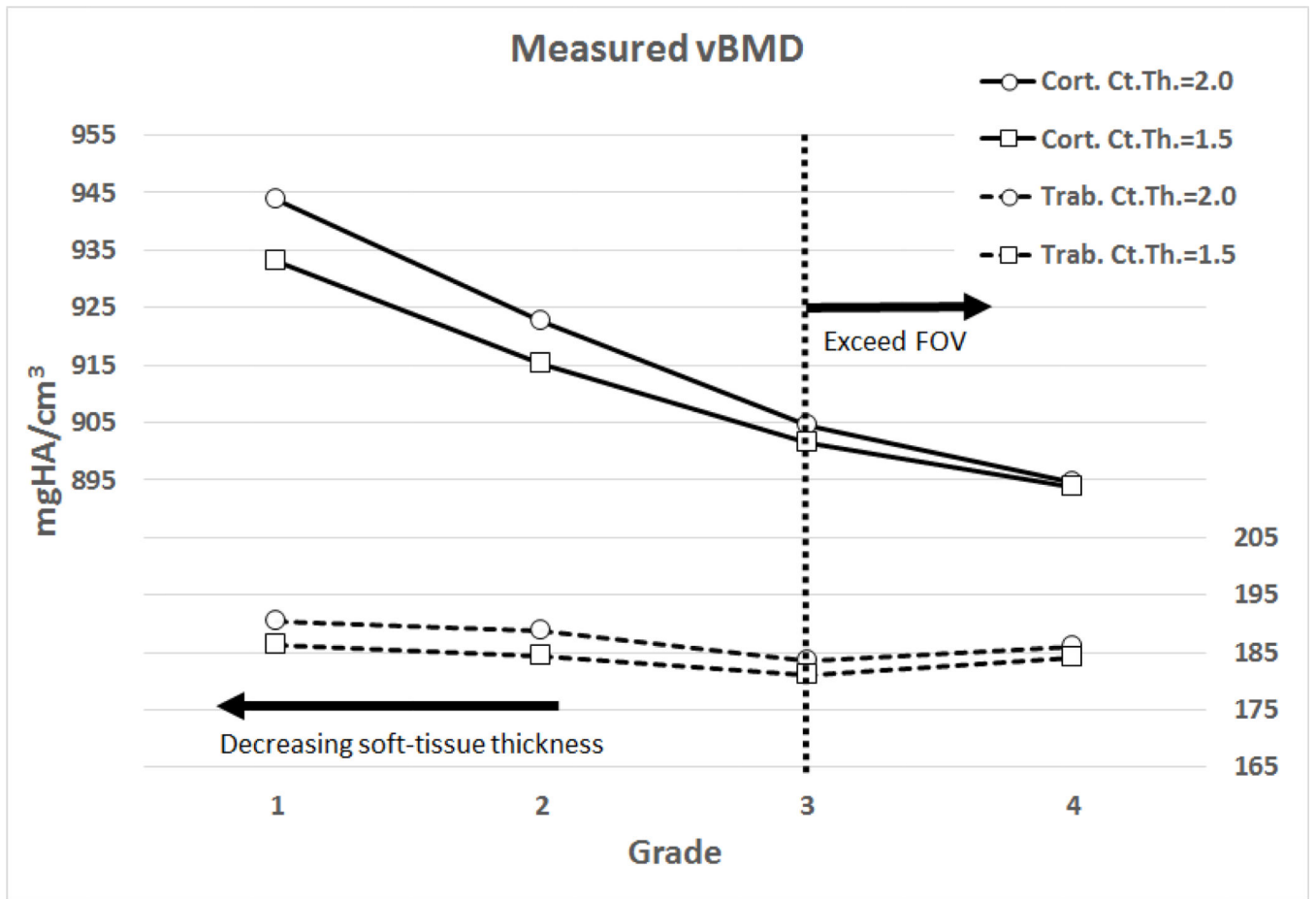


**Figure 5:** Trabecular and cortical vBMD is influenced by soft tissue volume and cortical thickness. Y-axis split to allow visualization of trabecular and cortical data together.

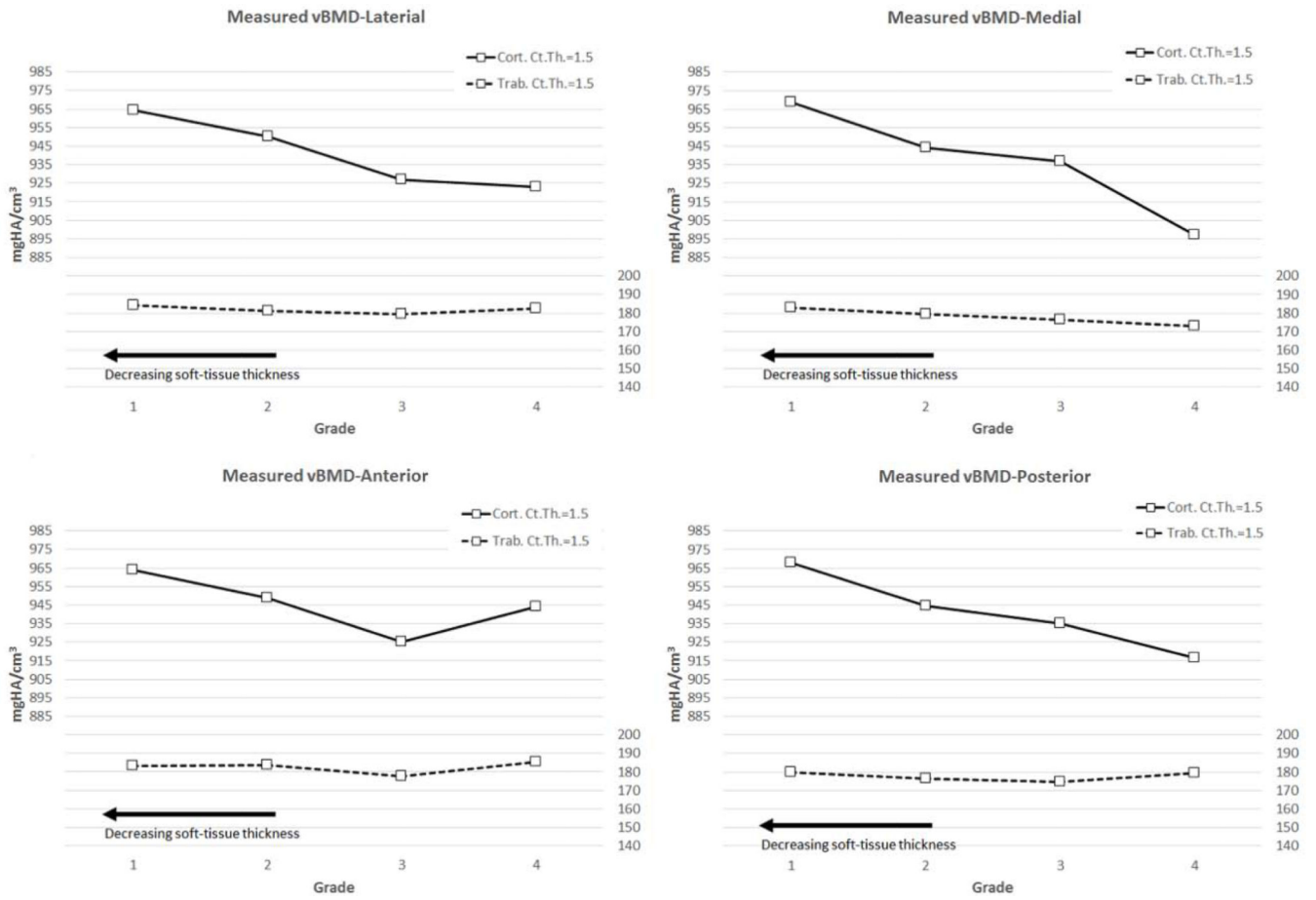


**Figure 6:** Trabecular and cortical vBMD for each anatomic quadrant. Y-axis split to allow visualization of trabecular and cortical data simultaneously.

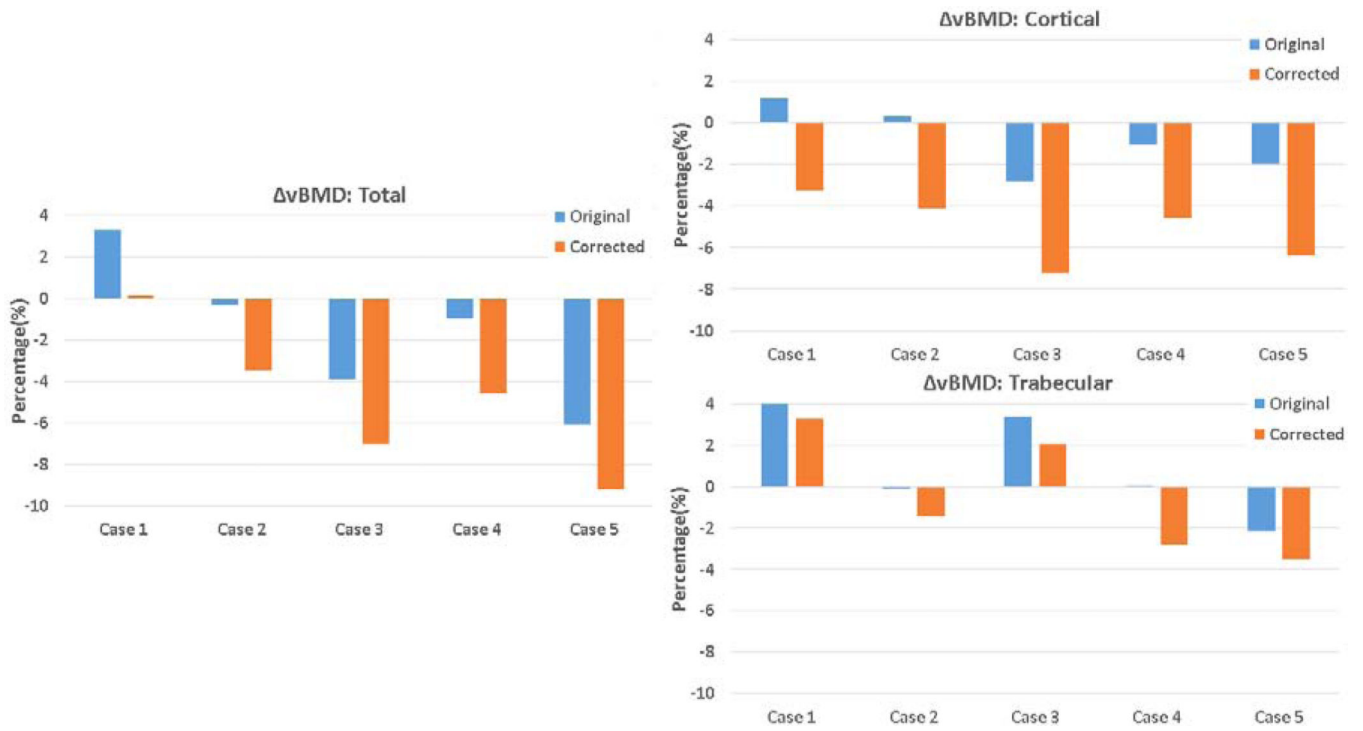


**Figure 7:** Originally reported and corrected 12-month longitudinal vBMD changes for individual RYGB patients.

**Table 1:**

Description of grading scheme, proximity of soft tissue to the edge of the field of view (FOV) at each grade, and thickness of phantom adipose tissue (fat layer) to achieve each configuration

<b>Grade</b>	<b>Proximity to FOV</b>	<b>Adipose tissue thickness</b>
Grade 1	within FOV	1.0 cm
Grade 2	at edge of FOV	1.5 cm
Grade 3	extending beyond FOV	2.0 cm
Grade 4	extending far beyond FOV	3.5 cm

Author Manuscript

Author Manuscript

Author Manuscript

Author Manuscript

**Table 2:**

Change in measured vBMD due to soft tissue reduction (  $vBMD_{soft\ tissue}$ ) in the phantom study.

		Phantom study: Change in measured vBMD due to soft tissue reduction			
		$vBMD_{soft\ tissue}$ (%)		$vBMD_{soft\ tissue}$ (%)	
		post: Grade 2		post: Grade 1	
		Ct.Th = 1.5mm	Ct.Th = 2mm	Ct.Th =1.5mm	Ct.Th = 2mm
pre: Grade 3	Total	1.8	2.5	3.6	4.3
	Trab	1.7	2.9	2.9	3.7
	Cort	1.5	2.0	3.5	4.4
pre: Grade 4	Total	1.3	2.4	3.1	4.3
	Trab	0.2	1.5	1.3	2.3
	Cort	2.4	3.1	4.4	5.5

**Table 3:**

Originally reported and corrected 12-month longitudinal vBMD changes for five RYGB patients. Paired t-test on corrected vBMD compared to original vBMD.

Clinical study : Comparison of original and corrected 12-month BMD change		
	Original vBMD(%)	Corrected vBMD(%)
Total	-1.6 ± 3.6	-4.8 ± 3.6 **
Trab	1.2 ± 2.8	-0.5 ± 3.0 *
Cort	-0.9 ± 1.6	-5.1 ± 1.7 **

\* : p<0.01

\*\* : p<0.0001

Author Manuscript

Author Manuscript

Author Manuscript

Author Manuscript